World Academy of Science, Engineering and Technology
International Journal of Transport and Vehicle Engineering
Vol:18, No:3, 2024

Investigating the Vehicle-Bicyclists Conflicts Using LIDAR Sensor Technology at Signalized Intersections

Alireza Ansariyar, Mansoureh Jeihani

Abstract**—**Light Detection and Ranging (LiDAR) sensors is capable of recording traffic data including the number of passing vehicles and bicyclists, the speed of vehicles and bicyclists, and the number of conflicts among both road users. In order to collect real-time traffic data and investigate the safety of different road users, a LiDAR sensor was installed at Cold Spring Ln – Hillen Rd intersection in Baltimore city. The frequency and severity of collected real-time conflicts were analyzed and the results highlighted that 122 conflicts were recorded over a 10-month time interval from May 2022 to February 2023. By employing an image-processing algorithm, a safety Measure of Effectiveness (MOE) aims to identify critical zones for bicyclists upon entering each respective zone at the signalized intersection. Considering the trajectory of conflicts, the results of analysis demonstrated that conflicts in the northern approach (zone N) are more frequent and severe. Additionally, sunny weather is more likely to cause severe vehicle-bike conflicts.

Keywords**—**LiDAR sensor, Post Encroachment Time threshold, vehicle-bike conflicts, measure of effectiveness, weather condition.

I. Introduction

As bicycle riding is becoming increasingly popular in most U.S. cities, the safety of this vulnerable group of road users is becoming increasingly of concern. In the interaction between bicycles and motorized vehicles, bicyclists as Vulnerable Road Users (VRUs) are at risk of traffic fatalities [1]. Various studies have shown that the frequency and severity of conflicts are reduced as the bike road is separated from other road users [1]-[5]. The presence of bicyclists may go unnoticed by car drivers due to distraction, malfunction, or system malfunction. The frequency of preventable deaths from bicycle transportation incidents in the U.S. increased by 16% in 2020 and has increased by 44% in the last decade, from 873 in 2011 to 1,260 in 2020. At the same time, from 536,412 injuries in 2011 to 325,173 injuries in 2020, the number of preventable nonfatal injuries has declined by 39%. However, the number of preventable nonfatal injuries did increase by 5% in 2020 compared to 2019 [6]. In order to better understand how bicyclists interact with other road users, especially motorized vehicles in urban areas, new technologies must be applied to collect both road users' behaviors. LIDAR sensor records the number, type, time, and longitudinal and lateral positions of conflicts between vehicles and bicyclists. LIDAR sensors have increasingly been used for recording real-time traffic data in recent years. In some studies [7]-[9], LIDAR sensor as a detached sensing technology has assisted few designs and planning works, precisely detecting and tracking bicyclists, and vehicles at intersections. In addition to collecting real-time traffic data (counts, speeds, conflicts, and trajectories), LIDAR sensors can assess the safety of various road users at intersections. It is important to identify critical zones of intersections between motorized vehicles and bicyclists in terms of frequency and severity of the conflicts and propose practical solutions for improving road safety.

Several infrastructure-based sensor technologies are available for traffic detection, including inductive loops, microwave radar, and CCTV (video cameras), which are probably the most popular. These sensor technologies are hindered by the inability to obtain trajectory-level data and low performance in the precise detection and tracking of vehicles and bicyclists. For long-term enhancement of evasive action by road users, a real-time collaborative system of infrastructure-mounted sensors is required. The LIDAR sensors are efficient infrastructure-based detection systems with much more processing and computing power can enhance the accuracy of traffic analysis, and can cover “illumination condition” issues [10] providing valid information regardless of the weather condition or recording video at night. LIDAR sensor records surrogate safety measures (SSM) including Post-Encroachment Time (PET) that is suitable tool in detecting dangerous near-crash situations between road users. PET is the main focus of our paper for motorized vehicle-bike conflicts. PET refers to the period between the time when the first vehicle last occupied a position and the time when the second vehicle subsequently occupied that same position [11]. PET equal to 0 indicates a collision and non-zero values indicate crash proximity. Higher PET values indicate a less severe crash, while lower PET values indicate a more severe crash. The state-of-the-art demonstrated that the collected PETs by a LIDAR sensor for vehicle-bike conflicts was not efficiently evaluated. To fill this gap, this paper investigates the critical zones in one of the hazardous signalized intersections in Baltimore city based on Baltimore police reports in terms of the frequency and severity of vehicle-bike conflicts. For doing so, based on the accuracy of LIDAR data at Cold Spring Ln – Hillen Rd intersection [12], a comprehensive analysis of vehicle-bike conflicts over a 10-month time interval is proposed. Following that, the paper

Alireza Ansariyar is Ph.D. candidate, Department of Transportation and Urban Infrastructure Systems (TUIS), Morgan State University, Baltimore, MD, USA (e-mail: alans2@morgan.edu).

Mansoureh Jeihani is Professor, TUIS, Morgan State University, Baltimore, MD, USA (e-mail: Mansoureh.jeihani@morgan.edu).

attempts to examine traffic and environmental characteristics, including traffic signal phasing and timing and the impact of weather on vehicle-bike conflict.

The remainder of this article is structured as follows: Section II: Literature Review, Section III: Research Methodology, Section IV: Analysis of Collected Vehicle-Bike Conflict Data by the LIDAR Sensor, Section V: Discussion, Section VI: Conclusion, and References.

II. Literature Review

In a crash between a bike and a vehicle, the cyclist is more likely to suffer injuries than the vehicle driver [13]. The published statistics in terms of bicyclist deaths by age and sex in the U.S. from 1975 to 2020 [14] highlighted the frequency of male bicyclists less than 20 years' old who were died in vehicle-bike conflicts decreased dramatically. The chart of female bicyclists younger than 20 years' old who died in vehicle-bike collisions experienced lower slope than male bicyclists. On the other hand, the chart of male and female bicyclists older than 20 years' old who were died in vehicle-bike conflicts experienced upward slopes. The report [14] also demonstrated that from 2010 to 2020, bicyclists without helmets were responsible for 59% of fatalities in vehicle-bike collisions, and bicyclists with helmets accounted for 16% of fatalities. Furthermore, summer is the peak riding season for bicyclists, which accounts for 33% of all bicyclist deaths in interaction with motorized vehicles in 2020. According to the diurnal distribution of bicyclist deaths in 2020, approximately 40% of fatalities occurred after 6 PM when the weather turns dark. Considering the importance of bicyclists safety as one of VRUs [15]-[18], it is important to investigate accurately the interaction between motorized vehicles and bicyclists on different types of roads. In recent years, various technologies were used to collect traffic data for vehicle-bike interaction e.g., bike or car simulators [1], [19]-[21], video recording or CCTVs [22]-[24], and LIDAR sensors [8], [25]-[27]. A LIDAR sensor, as a leading technology, can assist various research projects, especially those focusing on increasing pedestrian and bicycle safety. To save lives and build safer cities, intelligent road management and smarter traffic policies are essential. As a solution to this growing need, smart cities around the world have begun using LIDAR technology to monitor traffic and collect critical data to improve pedestrian and cyclist safety policies and infrastructure [28]. LIDAR technology can be an efficient solution to monitor vehicle-bike conflicts [7]. Globally, traffic injuries are the leading cause of bicyclists' death for individuals between the ages of 5 and 29 years [29]. Due to the accuracy of LIDAR sensors to collect conflict data [12], the resulting LIDAR data are used to generate 3D point clouds, which provide advanced 3D perception and situational awareness. In order to make data-driven decisions in real-time, these data are then analyzed using computer perception software. LIDAR sensors monitor and collect traffic data autonomously at intersections and roads, including how and when road users and vehicles use them. In the rain, snow, wind, dust, fog, bright sunlight, and very low light, 3D LIDAR sensors provide greater than 95% detection accuracy and 24/7 reliability [30]. It is possible for some LIDAR sensors to capture hundreds of points per second. With LIDAR, situational awareness can be enhanced beyond what can be achieved with cameras or manual data collection. LIDAR is a powerful and versatile technology that is capable of handling a variety of traffic monitoring applications, especially detecting bicyclists and pedestrians concealed in blind spots [31]. Traffic conflict measurements generally are continuous, and it is possible to model their severity as a continuous dependent variable by a transformation of the indicator [32]-[34] or the value of the indicator itself [35]. The literature declared that new technologies e.g., LIDAR has not been efficiently utilized for bicyclists safety detection in interaction with other vehicles. Due to filling the current gap in the state of the art, and based on the potential benefits of LIDAR technology to collect real-time conflict data, the present paper investigates the frequency and severity of vehicle-bike conflicts simultaneously, and analyze the critical zones for bicyclists at one of hazardous signalized intersections in Baltimore city, MD. Furthermore, the paper tries to evaluate the effect of traffic and environmental characteristics e.g., timing and phasing of traffic signal and the weather condition on the frequency and severity of vehicle-bike conflicts.

III. Research Methodology

E Cold Spring Ln-Hillen Rd intersection in Baltimore city, MD was equipped with a LIDAR sensor on the south-western side. As can be seen in Fig. 1, Cold Spring Ln is a two-way east-west road with three lanes in each direction, and Hillen Rd is a secondary north-south road with three lanes in each direction. The location of the LIDAR sensor is shown as a red circle in Fig. 1.

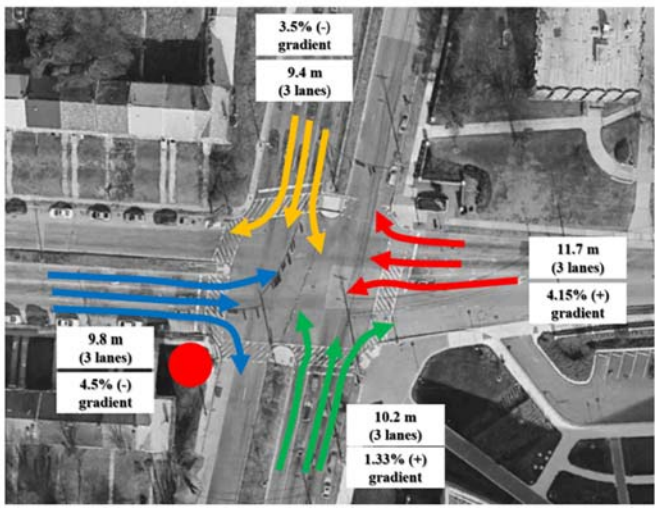

Fig. 1 Cold Spring Ln - Hillen Rd intersection [12]

Cold Spring Ln. is a 35-mile/hour speed and 1800 PCU/h capacity and Hillen Rd is a primary north-south road with 35 mile/hour speed and 1400 PCU/h capacity. To analyze the frequency of conflicts between motorized vehicles and bicyclists, a dashboard was designed to collect real-time PET

values, hourly conflict intervals, the speed of leading and following vehicles, and the longitudinal and lateral positions of conflicts. Machine-learning algorithms [12] are applied to the data collected from the roadside unit (RSU) in the intersection in order to process direct, left-turn, and right-turn movements. As a consequence, real-time flow charts are drawn to show vehicle volume/count, speed, conflicts, and signal timing. The raw data were processed and the highly accurate real-time traffic data (count, speed, conflicts, and jay-walking) were provided by using supervised machine learning [12]. The accuracy of collected PET data by LIDAR sensor was investigated with the recognized PETs by two installed Closed-Circuit Television (CCTVs) in the intersection – the same proposed methodology [36] – and the obtained PETs were analyzed frame by frame [37] to verify the highly accurate PET datasets. The real-time API that applied by LIDAR provides access to the frame data (location, class type and the tracking ID of each object within a frame), occupancy changes for each phase (virtual inductive loops that are called upon the presence of vehicles on the defined regions/loops), and phase changes at intersections (traffic light status) [37].

Image-processing toolbox in MATLAB software was used to provide a conflict heat map based on the longitudinal and lateral positions of conflicts. Additionally, the current phasing and timing of traffic signal patterns during AM peak, MD peak, and PM peak phases were imported into MATLAB code in order to determine the frequency of conflicts at each phase of the intersection during different hours of the day. The variables i.e., left-and right-turning trajectories of vehicles and bicyclists from the initial positions to conflict points, speed of left-turning and right-turning of the vehicles and bicyclists, zone of conflict, the entrance bicyclists volume to zone, weather, and the traffic signal timing and phasing were analyzed in order to specify the highly correlated variables to vehicle-bike conflicts at signalized intersections. It is worth mentioning that Excel, MATLAB, Python, and VeloView software [38] were used for the data analysis.

IV. Analysis of Collected Vehicle-Bike Conflict Data by the LIDAR Sensor

An initial analysis of vehicle-bike conflicts revealed 122 conflicts occurred between May 2022 and February 2023 (a 10-month interval). According to Fig. 2, 52% of total conflicts occurred after 5 PM on an hourly basis. There is a greater likelihood of conflict as the weather approaches sunset and afterward. The weather can have a significant impact on vehicle-bike conflicts depending on the time of day and the weather conditions, as shown in Fig. 2.

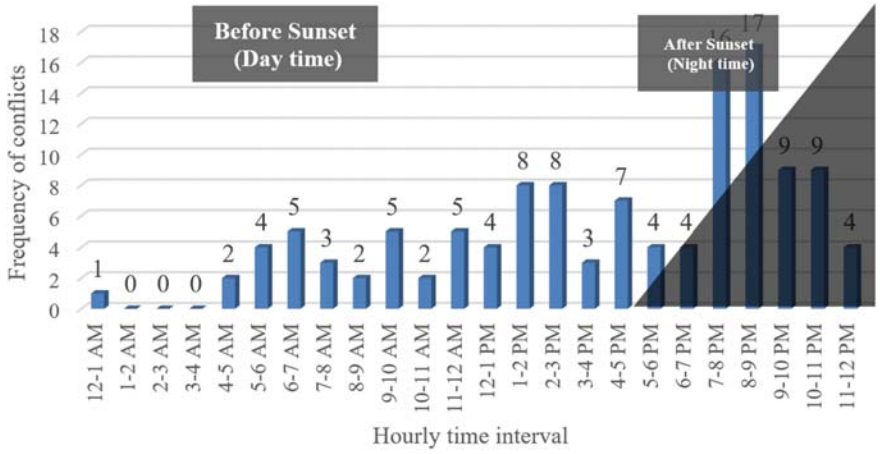

Fig. 2 Hourly frequency of vehicle-bike conflicts

Fig. 3 shows the monthly frequency of conflicts that were recorded from May to February, respectively.

Additionally, the conflicts decreased significantly over the summer (especially July and August), as the intersection was located close to Morgan State University, and the volume of vehicles decreased due to summer semester. Also, 9% of conflicts was collected in May three weeks before closing the public schools in Baltimore. The frequency and severity of conflicts over a 10-month time interval are shown in Fig. 4.

To effectively analyze the frequency and severity of conflicts, five zones including zone east (E), zone north (N), zone west (W), zone south (S), and zone center (C) were considered. Fig. 5 shows the location of each zone in the intersection. The LIDAR sensor can recognize the near-crash conflicts in a radius of 150 m. The LIDAR collected the longitudinal and lateral position of conflicts. Geographical coordinates of each conflicts were double-checked on Google Maps and open street maps to verify the exact location of conflict. The border of each zone was defined based on the location of stop lines and the border of the zones was determined in such a way to minimize the error of placing conflicts on the border between two zones.

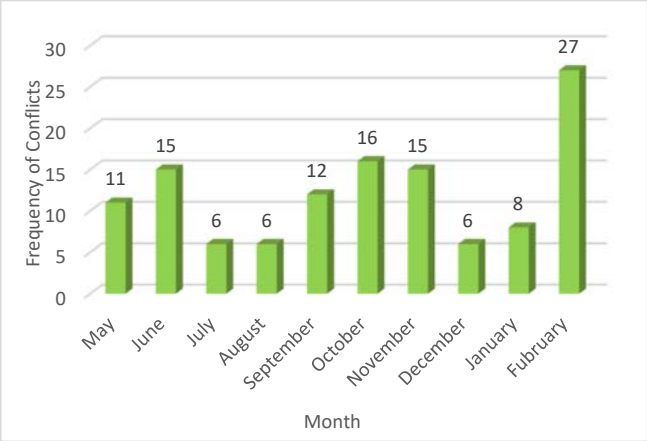

Fig. 3 Monthly frequency of vehicle-bike conflicts

Fig. 6 shows the frequency of conflicts in each zone. As can be seen in Fig. 6, 29%, 38%, 9%, 14%, and 11% of total conflicts were collected in zones E, N, W, S, and C, respectively. Furthermore, 66% of total conflicts were collected in northern and eastern approaches of the intersection (= zones N and E).

Vehicle-bike conflicts according to possible movements in the intersection were categorized. 12 possible movements can be defined by considering the approaches east (E), north (N), west (W), and south (S) as shown in Fig. 7, including EN, EW, ES, NW, NS, NE, WS, WE, WN, SE, SN, and SW. Fig. 7 demonstrates the frequency of vehicle-bike conflicts in each one of the 12 possible movements.

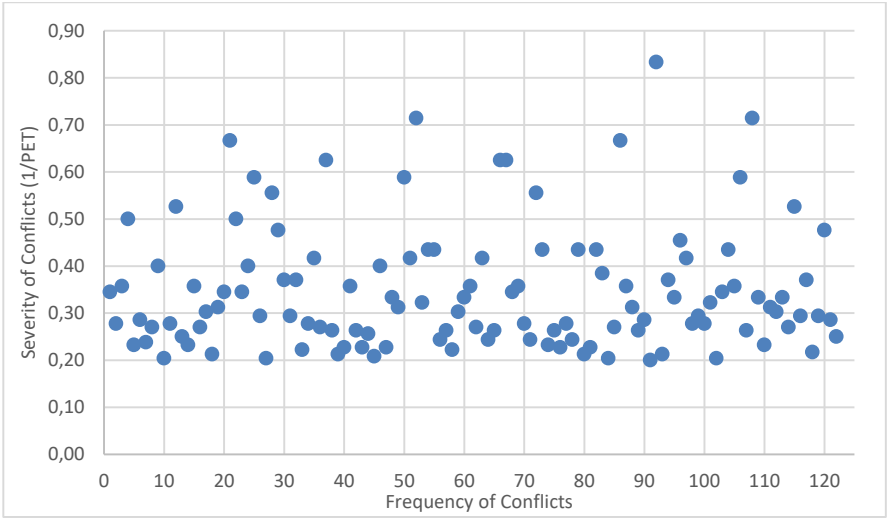

Fig. 4 The dispersion of the frequency and severity of the collected vehicle-bike conflicts

Fig. 5 The location of zones in the intersection

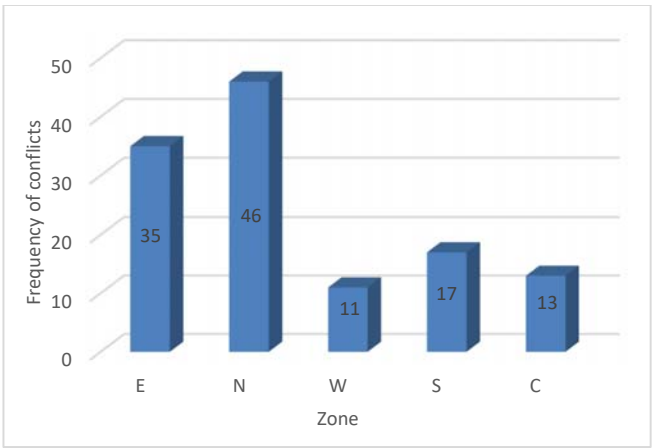

Fig. 6 Frequency of conflicts analysis in each zone

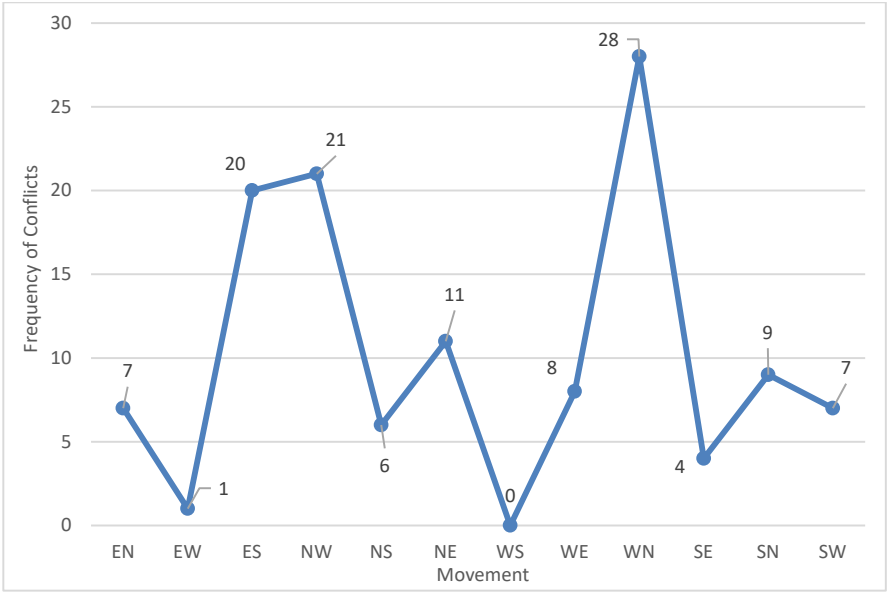

Fig. 7 Frequency of conflicts analysis in each movement

As can be seen in Fig. 7, 23%, 17%, and 16% of conflicts were occurred in WN (EBL), NW (SBR), and ES (WBL). Furthermore, based on the collected bike speed and vehicle speed in the conflict point, 39 conflicts were blamed on the bicyclist and 83 conflicts were blamed on the vehicle. According to the proposed PET categories in our previous study [12], four categories were investigated including 0 < PET < 0.7 as a serious conflict, 0.7 < = PET < 1.31 as a general conflict, 1.31 < = PET < 2.25 as a slight conflict, and 2.25 < = PET < = 5 as a potential conflict. The results of vehicle-bike PETs from LIDAR highlighted one general conflict (0.8%), 19 slight conflicts (15.6%), and 102 potential conflicts (83.6%) occurred during ten months' interval.

The LIDAR sensor was directly connected to a central computer in the controller cabinet of the intersection. The central computer can analyze normalizing of conflicts [12] considering the traffic volume of the intersection. A Machine Learning Algorithm was used for object detection and classification. A procedure was developed for roadside LIDAR data processing, including major steps of background, object clustering, identification of road user types, tracking road users in different data frames, and output of traffic trajectory data. The procedure of finding the objects by LIDAR sensor follows the following steps consecutively:

1. No traffic data frames are collected in time intervals when no traffic passes from different approaches to the intersection.
2. Multiple no-traffic data frames are aggregated to identify background objects and removed them from LIDAR data frames.
3. In order to create the elevation-azimuth matrix, the 3D point clouds are first converted into spherical coordinates. To store range, azimuth, and intensity information, the raw LIDAR data were rearranged into the new data structure. Using intensity channel pattern recognition as described [39], the LIDAR data are decomposed into low-rank backgrounds and sparse foregrounds.
4. According to the reflectivity of the object and the wavelength that the LIDAR uses, a position packet and a data packet are created. Position packets are known as GPS packets, and data packets contain information about distance and intensity. LIDAR systems use spherical coordinates initially and then transform spherical data to XYZ coordinates.
5. Moving points are clustered so that they can be easily distinguished from the foreground and background. By using an azimuth-height background filtering method proposed by [40], an azimuth-height table is developed. The height of each point with the height of backgrounds is compared to recognize and then classify road users and non-road users in different data frames.

The accuracy of using these algorithms when counting vehicles is 97.5% and the accuracy of measuring speed ranges from 92% to 96%, depending on the vehicle's average moving speed [39], [41]. The frequency of conflicts in terms of leading and following vehicles was analyzed. Table I shows the frequency of leading conflicts (motorized vehicles as leading) in different zones. Additionally, Table II shows the total frequency of following conflicts (motorized vehicles as following). Table II shows the frequency of conflicts in each approach (Eastern, Western Northern, and Southern) of the intersection based on leading or following vehicles.

TABLE I
FREQUENCY OF LEADING CONFLICTS IN DIFFERENT ZONES AND BASED ON DIFFERENT APPROACHES

ZONE	Leading Vehicles											
	EN	EW	ES	NW	NS	NE	WS	WE	WN	SE	SN	SW
E	2	1	4	0	0	6	0	3	0	1	0	0
N	1	0	0	6	2	2	0	0	3	0	3	0
W	0	0	0	3	0	0	0	0	1	0	0	0
S	0	0	8	0	0	0	0	0	0	0	1	1
C	2	0	1	0	0	0	0	1	0	0	0	1

TABLE II
FREQUENCY OF FOLLOWING CONFLICTS IN DIFFERENT ZONES AND BASED ON DIFFERENT APPROACHES

ZONE	Following Vehicles											
	EN	EW	ES	NW	NS	NE	WS	WE	WN	SE	SN	SW
E	2	1	6	0	0	3	0	2	0	2	0	0
N	3	0	0	8	6	4	0	0	4	0	5	0
W	0	0	0	1	0	0	0	3	2	0	0	1
S	0	0	2	0	0	0	0	0	0	0	2	4
C	0	0	1	0	0	0	0	1	6	0	0	0

In order to analyze the frequency of conflicts in each phase of the intersection, the timing and phasing of the intersection in different daily time intervals were collected. The results highlighted eight phases and three timing patterns at morning (AM), mid-day (MD), and afternoon (PM). Image processing in MATLAB software was used to analyze the frequency of conflicts in each phase. For each zone in each phase, the frequency of conflicts was determined based on the pattern of timing and phasing of the intersection. Table III shows the timing patterns of traffic signal in the intersection.

TABLE III
TIMING AND PHASING PATTERN OF THE TRAFFIC SIGNAL

Phase	Min green time	Gap (sec)	Max green time (sec)	Yellow time (sec)	AM pattern[1]	MD pattern[2]	PM pattern[3]
ϕ1	8	2	20	4.6	19	17	21
ϕ2	10	3	70	4.6	70	45	76
ϕ3	7	1.5	20	4.1	21	17	15
ϕ4	10	3	50	4.5	50	41	48
ϕ5	7	1.5	20	4.6	19	22	15
ϕ6	10	3	70	4.6	70	40	82
ϕ7	8	1.5	20	4.1	21	22	27
ϕ8	10	3	50	4.5	50	36	36

1. Green time of phase (sec) in morning peak hour time interval
2. Green time of phase (sec) in mid-day peak hour time interval
3. Green time of phase (sec) in afternoon peak hour time interval

Fig. 8 shows the eight phases of the traffic signal in the intersection.

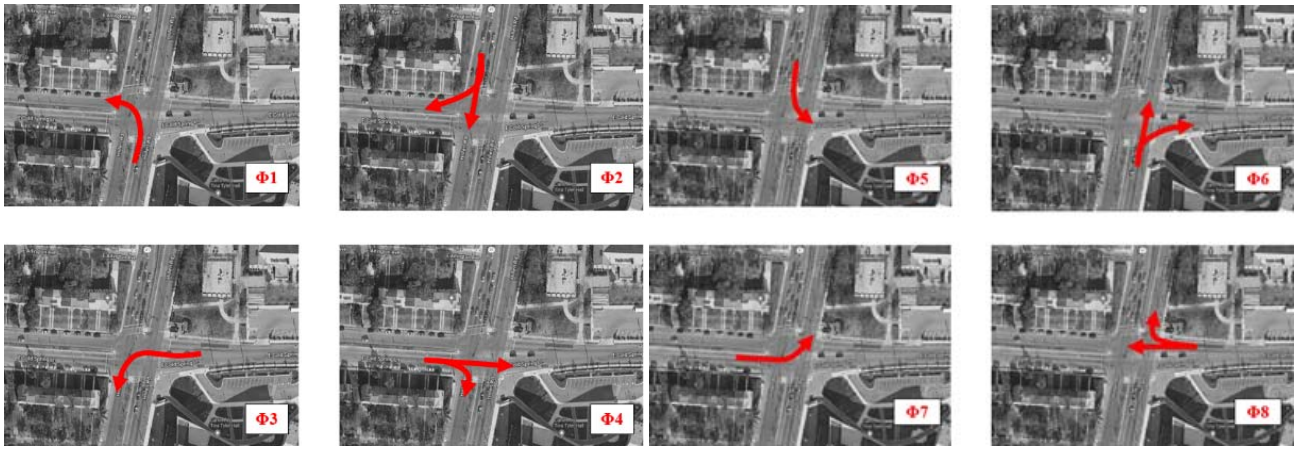

Fig. 8 Phasing of traffic signal in the intersection

As the output of image processing, Table IV shows the frequency of conflicts in each zone and by each phase of the traffic signal. As can be seen in Table IV, a significant number of conflicts was collected in phase 3 (ES), phase 5 (NE), and phase 2 (NS & NW).

TABLE IV
FREQUENCY OF CONFLICTS IN EACH PHASE OF TRAFFIC SIGNAL

Zone	ϕ1	ϕ2	ϕ3	ϕ4	ϕ5	ϕ6	ϕ7	ϕ8	SUM
E	0	0	15	6	6	4	0	4	**35**
N	0	9	0	0	14	6	13	4	**46**
W	2	3	0	2	0	0	3	1	**11**
S	2	6	4	2	0	3	0	0	**17**
C	0	3	4	1	2	0	3	0	**13**

The severity of conflicts was analyzed based on sum of numerical values of PETs in each zone. The lower the numerical value of PET shows the higher severity of conflicts. Therefore, higher 1/PET shows the higher severity of conflicts. The LIDAR sensor collects "near-crash" conflict data so that for each pair of objects with a conflict, PET is calculated as the time between the moment the first road user leaves the conflict point and the moment the second reaches the same point. The type of vehicle (personal car, truck, or bus) is recognized by LIDAR, and the mass of leading or following vehicles is taken into account to provide PET values. Hence, 1/PET shows the severity of near-crash conflicts. Based on the size and mass of leading or following vehicles, the LIDAR sensor can estimate the severity of conflicts (by lower numerical PET value).

As shown in Table V, column "average daily 1/PET" shows the ADT of PETs for each zone.

TABLE V
SEVERITY OF CONFLICTS IN EACH ZONE

Zone	Sum of frequency of conflicts	Sum (1/PET)	Average Speed (km/hr)	Average Daily 1/PET
E	35	12.41	27.3	0.0408
N	46	16.17	26.1	0.0532
W	11	3.82	21.7	0.0125
S	17	5.82	25.1	0.0191
C	13	4.12	23.7	0.0135

In Table V, a significant proportion of conflicts occurred in zones N and E, as expected since 66% of total conflicts occurred

in these zones. In order to specify the safety condition of bicyclists in different approaches to the intersection, sum 1/PET was compared to the passing bicyclists volume. The Average Daily Traffic (ADT) of bicyclists for time interval May 2022 to February 2023 was analyzed. The results are shown in Table VI.

TABLE VI
THE RESULTS OF PASSING BICYCLIST VOLUME FROM DIFFERENT INTERSECTION APPROACHES

Month	Passing bike volume from zone E	Passing bike volume from zone N	Passing bike volume from zone W	Passing bike volume from zone S	Sum of bicyclists volume	ADT of bicyclists
May 2022	111	96	161	122	490	16
June 2022	163	53	173	69	458	15
July 2022	762	73	206	69	1110	36
August 2022	314	96	221	172	803	28
September 2022	491	172	296	308	1267	42
October 2022	327	128	125	303	883	30
November 2022	229	82	86	171	568	19
December 2022	85	44	53	90	272	9
January 2023	129	59	82	128	398	13
February 2023	196	73	99	184	552	20
SUM	2807	876	1502	1616	6801	228

The entrance volume of bicyclists to zone C should be determined based on the trajectory of bicyclists. Based on the bicyclists' trajectory, 6678 bicyclists pass through zone C. Considering the entrance movement (e.g., EW, EN, WE, WN, …) to each zone, a Measure of Effectiveness (MOE) as can be seen in (1) was proposed. The MOE as shown in Table VII specifies the severity of conflicts relative to entrance bicyclists volume.

$$MOE = \frac{Average\ Daily\ (\frac{1}{PET})}{Entrance\ bicyclists\ volume\ to\ zone} \quad (1)$$

TABLE VII
THE MOE RESULTS FOR THE FREQUENCY AND SEVERITY OF VEHICLE-BIKE CONFLICTS

Zone	Sum of frequency of conflicts	Sum (1/PET)	Average Daily 1/PET	Entrance bicyclists Volume to Zone	MOE $*10^5$	Critical Zone
E	35	12.41	0.0408	2807	1.45	*
N	46	16.17	0.0532	876	6.07	*
W	11	3.82	0.0125	1502	0.83	
S	17	5.82	0.0191	1616	1.18	
C	13	4.12	0.0135	6678	0.20	

Fig. 9 Heat map of vehicle-bike conflicts over a 10-month time interval

As can be seen in Table VII, zones N, and E are critical zones in terms of vehicle-bike conflicts. Additionally, zone N demonstrates considerable severity of conflicts. Consequently, the probability of injury or fatalities in zone N is higher than the other zones. The heat map of vehicle-bike conflicts frequency and severity based on the proposed MOE over a ten-month time interval is shown in Fig. 9. The northern approach to the intersection shows significant vehicle-bike conflicts, as shown in Fig. 9.

V. DISCUSSION

Variables e.g., left-and right-turning trajectories of vehicles and bicyclists from the initial positions to conflict points, speed of left-turning and right-turning of the vehicles and bicyclists, time and distance length of vehicles and bicyclists trajectories, hourly time interval of vehicle-bike conflict, zone of conflict, the entrance bicyclists volume to zone, weather, and the performance of traffic signal timing and phasing were analyzed to specify the accuracy and severity of collected PETs by LIDAR in critical zones. Zone of conflict [42], [43], time interval of conflict [44], [45], and weather [46]-[48] have been identified as effective factors in conflicts between motorized vehicles and other road users. On the same line with previous studies [49]-[51], this paper investigated the effective independent variables in vehicle-bike conflicts. Hereupon, the results of statistical analysis, as shown in Table VII, specified zones N, and E are critical zones for bicyclists. Zones N and E are in close proximity of Morgan State University campuses. Hence, these two zones are expected to see significant traffic conflicts involving vehicles and bikes. As shown in Fig. 2, 52% of total conflicts occurred after 5 PM on an hourly basis. Vehicle-bike conflicts may be affected by the light condition of the day and the weather condition. Therefore, the purpose of this section is to investigate whether weather conditions have any effect on vehicle-bike conflicts. The results of weather condition analysis are shown in Table VIII.

As shown in Table VIII, on sunny days, vehicle-bike conflicts were more severe than in cloudy weather, despite the

fact that their frequency was 10.8% less than cloudy days. The results of vehicle-bike conflicts frequencies in different weather conditions and based on zones are shown in Table IX.

TABLE VIII
FREQUENCY OF VEHICLE-BIKE CONFLICTS IN DIFFERENT WEATHER CONDITIONS

Weather	Frequency of Vehicle-bike conflicts	Sum (1/PET)
Cloudy	51	17.01
Sunny	46	17.54
Rainy	25	7.8

TABLE IX
FREQUENCY OF VEHICLE-BIKE CONFLICTS IN EACH ZONE IN DIFFERENT WEATHER CONDITIONS

Zone/weather	Cloudy	Sunny	Rainy	SUM
E	12	15	8	35
N	16	17	13	46
W	6	5	0	11
S	8	6	3	17
C	9	3	1	13
SUM	51	46	25	122

Table X shows the severity of vehicle-bike conflicts in different weather conditions in each zone.

TABLE X
SEVERITY OF VEHICLE-BIKE CONFLICTS IN EACH ZONE IN DIFFERENT WEATHER CONDITIONS

Zone/weather	Cloudy	Sunny	Rainy	SUM (1/PET)
E	3.98	5.55	2.87	12.41
N	4.95	7.45	3.76	16.17
W	2.11	1.71	0	3.82
S	2.96	1.99	0.88	5.82
C	3	0.84	0.28	4.12
SUM	17.01	17.54	7.8	42.35

As shown in Table X, conflicts in zone N are always more severe on sunny, cloudy, and rainy days than in other zones. In accordance with Table XII results, zone N is the critical zone of the intersection in terms of the frequency, severity, and MOE. A comparison of vehicle-bike conflicts in terms of frequency (Table IX) and severity (Table X) reveals an average of 0.309, 0.438, and 0.289 for each conflict occurring in zone N on cloudy, sunny, and rainy days, respectively. The fatalities and injuries caused by vehicle-bike conflicts are more likely to happen on sunny, cloudy, and rainy days in zone N. Different reasons including the proximity to Morgan State University's main campus, the gradient of the road in this zone, the illegal crossing of bicyclists in that zone, and the inability of motorized drivers to recognize bicyclists in that zone may increase the probability of vehicle-bike collisions in zone N.

VI. CONCLUSIONS

Intelligent systems have paved the way to new innovative opportunities for improving the safety of transportation networks. LIDAR sensors have emerged in recent years as one of the most innovative technologies available, allowing users to interact with and analyze traffic data in stunning detail. Due to the extent of data delivered by LIDAR technology, existing data collection problems such as poor weather conditions, and routes with restricted access can be resolved. In order to access the extent of the data obtained by LIDAR technology, a Velodyne LIDAR sensor was installed on the south-western side of E Cold Spring Ln – Hillen Rd intersection in Baltimore city, MD. This intersection was selected due to its considerable daily traffic volume, its close proximity to Morgan State University, and its density of residential land-uses in the surrounding area. The count vehicle and bike volumes data, speed data, and the frequency and severity of conflicts in time interval May 1st, 2022 to February 28th, 2023 (a 10-month time interval) were analyzed. The results specified 122 vehicle-bike conflicts. In order to analyze the conflicts, the internal area of the intersection was divided into five zones. In each zone, the frequency and severity of conflicts were analyzed based on two ways including leading and following vehicles conflicts, and in different phases of the traffic signal. An innovative image-processing algorithm was developed in MATLAB software to specify the frequency of vehicle-bike conflicts in different daily controlling patterns of the traffic signal. The results of leading and following vehicles conflicts (Tables I and II) demonstrated that the movements ES (= 13 conflicts), NW (= 9 conflicts), and NE (= 8 conflicts) are critical leading movements. Additionally, the movements WN (= 12 conflicts), ES (= 9 conflicts), and NW (= 9 conflicts) are critical following movements. As shown in Table IV, the results of the frequency of conflicts in different phases of the traffic signal highlighted that a significant number of conflicts was collected in ϕ3 (ES), ϕ5 (NE), and ϕ2 (NS & NW). The results of innovative safety Measure of Effectiveness (MOE) as shown in Table VII specified that zones N, E, and S are critical zones in terms of vehicle-bike conflicts. Furthermore, zone N exhibits considerable severity of vehicle-bike conflicts. Therefore, zone N is more likely to experience injuries or fatalities than other zones.

Variables e.g., left-and right-turning trajectories of vehicles and bicyclists from the initial positions to conflict points, speed of left-turning and right-turning of the vehicles and bicyclists, time and distance length of vehicles and bicyclists trajectories, hourly time interval of vehicle-bike conflict, zone of conflict, the entrance bicyclists volume to zone, weather, and the performance of traffic signal timing and phasing were analyzed to specify the accuracy and severity of collected PETs by LIDAR in critical zones. Vehicle-bike conflicts tend to be aggravated by weather conditions, according to the results of trajectories. According to Table VIII, vehicle-bike conflicts were more severe on sunny days than on cloudy days despite their frequency being 10.8% lower on sunny days. Moreover, conflicts in zone N are always more severe on sunny, cloudy, and rainy days than in other zones. Consequently, our research yielded the following contributions:

- Analysis of vehicle-bike conflicts at a signalized intersection in Baltimore City with a high fatality rate for pedestrians and cyclists.
- Analysis of vehicle-bike conflicts based on the movement in each approach in each zone, leading and following vehicles, and in different phases of the traffic signal by an innovative image processing algorithm.

- Developing a MOE for vehicle-bike conflicts that take into account the frequency and severity of conflicts, as well as the bicyclist's volume entering the zone.
- Analysis of the trajectory of motorized vehicles and bicyclists to determine the effect of weather on the frequency and severity of vehicle-bike conflicts.

The main limitation of the study is its confined time interval of 10-months. As a future work, the authors are interested in working on statistical models e.g., Hierarchical Poisson Regression (HPR), logistic regression models, and multinomial logit models. The paper helps decision-makers in Baltimore city to recognize the spots with the highest potential for vehicle-bike conflicts, and improve the timing and phasing of the traffic signal in order to decrease the frequency and the severity of vehicle-bike conflicts. The conclusions of the paper provide a useful reference for researchers when they select a suitable model to describe the frequency and severity of vehicle-bike conflicts in signalized intersections in other contexts.

ACKNOWLEDGEMENT

This study was supported by the Urban Mobility & Equity Center, a Tier 1 University Transportation Center of the U.S. Department of Transportation University Transportation Centers Program at Morgan State University.

DISCLOSURE OF INFORMATION AND CONFLICTS OF INTEREST

The authors declare that they have no conflict of interest.

REFERENCES

[1] Ansariyar, A., et al., Investigating the Traffic Behavior of Bicyclists in Interaction with Car Users on Shared bike lanes without physical barriers. Transportation Research Board 102nd Annual Meeting Transportation Research Board, 2023. https://trid.trb.org/view/2117768.
[2] Zangenehpour, S., et al., Are signalized intersections with cycle tracks safer? A case–control study based on automated surrogate safety analysis using video data. Accident Analysis & Prevention, 2016. 86: p. 161-172.
[3] Thomas, B. and M. DeRobertis, The safety of urban cycle tracks: A review of the literature. Accident Analysis & Prevention, 2013. 52: p. 219-227.
[4] Lusk, A.C., et al., Risk of injury for bicycling on cycle tracks versus in the street. Injury prevention, 2011. 17(2): p. 131-135.
[5] Teschke, K., et al., Route infrastructure and the risk of injuries to bicyclists: a case-crossover study. American journal of public health, 2012. 102(12): p. 2336-2343.
[6] Council, N.S. Bicycle Deaths. 2022; Available from: https://injuryfacts.nsc.org/home-and-community/safety-topics/bicycle-deaths/.
[7] Wang, D.Z., I. Posner, and P. Newman. What could move? finding cars, pedestrians and bicyclists in 3d laser data. in 2012 IEEE International Conference on Robotics and Automation. 2012. IEEE.
[8] Nateghinia, E., et al., A LiDAR-based methodology for monitoring and collecting microscopic bicycle flow parameters on bicycle facilities. Transportation, 2022: p. 1-25.
[9] Wu, J., et al., Automatic vehicle classification using roadside LiDAR data. Transportation Research Record, 2019. 2673(6): p. 153-164.
[10] Mukhtar, A., L. Xia, and T.B. Tang, Vehicle detection techniques for collision avoidance systems: A review. IEEE transactions on intelligent transportation systems, 2015. 16(5): p. 2318-2338.
[11] FHWA, Surrogate Safety Assessment Model and Validation: Final Report. 2008: U.S. Department of Transportation.
[12] Ansariyar, A. and A. Taherpour, Statistical Analysis of Vehicle-Vehicle Conflicts with a LIDAR Sensor in a Signalized Intersection. Advanced in transportation studies 2023(60): p. 87-106.
[13] NHTSA. Overview of Bicycle Safety. 2020; Available from: https://www.nhtsa.gov/road-safety/bicycle-safety.
[14] Safety, I.I.f.H. Fatality Facts 2020 for Bicyclists. 2020; Available from: https://www.iihs.org/topics/fatality-statistics/detail/bicyclists.
[15] Ptak, M., Method to assess and enhance vulnerable road user safety during impact loading. Applied Sciences, 2019. 9(5): p. 1000.
[16] Otte, D., M. Jänsch, and C. Haasper, Injury protection and accident causation parameters for vulnerable road users based on German In-Depth Accident Study GIDAS. Accident Analysis & Prevention, 2012. 44(1): p. 149-153.
[17] Rahman, M.S., et al., Applying machine learning approaches to analyze the vulnerable road-users' crashes at statewide traffic analysis zones. Journal of safety research, 2019. 70: p. 275-288.
[18] Vanlaar, W., et al., Fatal and serious injuries related to vulnerable road users in Canada. Journal of safety research, 2016. 58: p. 67-77.
[19] Boda, C.-N., et al., Modelling how drivers respond to a bicyclist crossing their path at an intersection: How do test track and driving simulator compare? Accident Analysis & Prevention, 2018. 111: p. 238-250.
[20] Nazemi, M., et al., Studying bicyclists' perceived level of safety using a bicycle simulator combined with immersive virtual reality. Accident Analysis & Prevention, 2021. 151: p. 105943.
[21] Rakha, H., et al., Bicyclist Longitudinal Motion Modeling. 2022.
[22] Mehta, K., B. Mehran, and B. Hellinga, Evaluation of the passing behavior of motorized vehicles when overtaking bicycles on urban arterial roadways. Transportation Research Record, 2015. 2520(1): p. 8-17.
[23] Johnson, M., et al., Cyclists and open vehicle doors: Crash characteristics and risk factors. Safety science, 2013. 59: p. 135-140.
[24] Fonseca-Cabrera, A.S., et al., Micromobility Users' Behaviour and Perceived Risk during Meeting Manoeuvres. International journal of environmental research and public health, 2021. 18(23): p. 12465.
[25] Woongsun, J. and R. Rajamani. A novel collision avoidance system for bicycles. in 2016 American Control Conference (ACC). 2016.
[26] Blankenau, I., et al., Development of a low-cost LiDAR system for bicycles. 2018, SAE Technical Paper.
[27] Xie, Z. and R. Rajamani. On-bicycle vehicle tracking at traffic intersections using inexpensive low-density LiDAR. in 2019 American Control Conference (ACC). 2019. IEEE.
[28] Thakur, R., Scanning LIDAR in Advanced Driver Assistance Systems and Beyond: Building a road map for next-generation LIDAR technology. IEEE Consumer Electronics Magazine, 2016. 5(3): p. 48-54.
[29] Organization, W.H., Road safety (Road traffic injuries). 2020. https://www.who.int/news-room/fact-sheets/detail/road-traffic-injuries
[30] Wu, J., H. Xu, and J. Zheng. Automatic background filtering and lane identification with roadside LiDAR data. in 2017 IEEE 20th International Conference on Intelligent Transportation Systems (ITSC). 2017. IEEE.
[31] Becker, G. How LiDAR is Making Roads Safer for Pedestrians and Cyclists. 2021; Available from: https://www.masstransitmag.com/technology/article/21236672/how-LiDAR-is-making-roads-safer-for-pedestrians-and-cyclists.
[32] Kiefer, R.J., D.J. LeBlanc, and C.A. Flannagan, Developing an inverse time-to-collision crash alert timing approach based on drivers' last-second braking and steering judgments. Accident Analysis & Prevention, 2005. 37(2): p. 295-303.
[33] Ismail, K., T. Sayed, and N. Saunier, Methodologies for aggregating indicators of traffic conflict. Transportation research record, 2011. 2237(1): p. 10-19.
[34] Zheng, L. and K. Ismail, A generalized exponential link function to map a conflict indicator into severity index within safety continuum framework. Accident Analysis & Prevention, 2017. 102: p. 23-30.
[35] Zheng, L., T. Sayed, and F. Mannering, Modeling traffic conflicts for use in road safety analysis: A review of analytic methods and future directions. Analytic methods in accident research, 2021. 29: p. 100142.
[36] Bluecity. LiDAR Sensor Accuracy of Bluecity LiDAR-Based Traffic Monitoring System. 2021; Available from: https://bluecity.ai/resources/accuracy-white-paper/.
[37] Bluecity, Data Structure by LIDAR technology. 2021.
[38] Jacquet, B. VeloView: The Velodyne LiDAR Viewer based on Paraview LiDAR. 2021; Available from: https://www.paraview.org/veloview/.
[39] Bombardier, R.d.P.a.R.J.A., Stop Line Detection Study. 2022.
[40] Zhao, J., et al. Azimuth-Height background filtering method for roadside LiDAR data. in 2019 IEEE Intelligent Transportation Systems Conference (ITSC). 2019. IEEE.
[41] Bluecity, Bluecity LIDAR data evaluation report. 2022.
[42] Pirdavani, A., et al. A Simulation-Based Traffic Safety Evaluation of Signalized and Un-Signalized Intersections. in Proceedings of the 15th International Conference Road Safety on Four Continents. 2010.

[43] Chen, A.Y., et al., Conflict analytics through the vehicle safety space in mixed traffic flows using UAV image sequences. Transportation Research Part C: Emerging Technologies, 2020. 119: p. 102744.
[44] Workineh, A.A., Analysis of the relationship between traffic conflicts and level of service at four-legged, signalized intersections in Sacramento. 2014, California State University, Sacramento.
[45] Lu, G., et al., Relationship Between Road Traffic Accidents and Conflicts Recorded by Drive Recorders. Traffic Injury Prevention, 2011. 12(4): p. 320-326.
[46] Zeng, Q., et al., Investigating the impacts of real-time weather conditions on freeway crash severity: a Bayesian spatial analysis. International journal of environmental research and public health, 2020. 17(8): p. 2768.
[47] Jiang, R., et al., Determining an Improved Traffic Conflict Indicator for Highway Safety Estimation Based on Vehicle Trajectory Data. Sustainability, 2021. 13(16): p. 9278.
[48] Saha, S., et al., Adverse weather conditions and fatal motor vehicle crashes in the United States, 1994-2012. Environmental health, 2016. 15(1): p. 1-9.
[49] Rakha, H., et al., Bicyclist Longitudinal Motion Modeling, U.S. Department of Transportation (U.S. DOT) report, https://papers.ssrn.com/sol3/papers.cfm?abstract_id=4377722.
[50] Ansariyar, A. and A. Taherpour, Investigating the accuracy rate of vehicle-vehicle conflicts by LIDAR technology and microsimulation in VISSIM and AIMSUN. Advanced in transportation studies 2023(61): p. 37-52.
[51] Ansariyar, A., Ardeshiri, A., Jeihani, M., Investigating the collected vehicle-pedestrian conflicts by a LIDAR sensor based on a new Post Encroachment Time Threshold (PET) classification at signalized intersections. Advanced in transportation studies 2023(61): p. 103-118.